

The Low Column Density Lyman-alpha Forest

Nickolay Y. Gnedin^{1,2} and Lam Hui¹

Received _____; accepted _____

arXiv:astro-ph/9608156v1 24 Aug 1996

¹Department of Physics, Massachusetts Institute of Technology, Cambridge, MA 02139;
e-mail: *gnedin@arcturus.mit.edu*, *lhui@space.mit.edu*

²Princeton University Observatory, Peyton Hall, Princeton, NJ 08544

ABSTRACT

We develop an *analytical* method based on the lognormal approximation to compute the column density distribution of the Lyman-alpha forest in the low column density limit. We compute the column density distributions for six different cosmological models and found that the standard, *COBE*-normalized CDM model cannot fit the observations of the Lyman-alpha forest at $z = 3$. The amplitude of the fluctuations in that model has to be lowered by a factor of almost 3 to match observations. However, the currently viable cosmological models like the slightly tilted *COBE*-normalized CDM+ Λ model, the CHDM model with $\Omega_\nu = 0.2$, and the low-amplitude Standard CDM model are all in agreement with observations, to within the accuracy of our approximation, for the value of the cosmological baryon density at or higher than the old Standard Big Bang nucleosynthesis value of $\Omega_b h^2 = 0.0125$ for the currently favored value of the ionizing radiation intensity. With the low value for the baryon density inferred by Hogan & Rugers (1996), the models can only marginally match observations.

Subject headings: intergalactic medium – quasars: absorption lines – cosmology: large-scale structure of Universe

1. Introduction

The Lyman-alpha forest, numerous weak hydrogen absorption lines in the spectra of distant quasars, have been the focus of extensive study for more than two decades. Recent cosmological hydrodynamic simulations greatly advance our understanding of it and allow unambiguous confrontation between observations with theoretical models (Cen et al. 1994; Miralda-Escude et al. 1995; Hernquist et al. 1996; Zhang et al. 1996).

Numerical simulations show that the Lyman-alpha forest forms as a result of absorption of the quasar light by neutral hydrogen in inhomogeneities on small scales very much like the Lyman limit systems, arising from absorption by galaxies on larger scales. One of the predictions of such models is that the low column density Lyman-alpha forest ($N_{\text{HI}} \lesssim 10^{14} \text{ cm}^{-2}$) resides in regions of low overdensity and even underdense regions of the universe. While higher column density Lyman-alpha systems³ form in significantly overdense regions ($\delta \equiv \delta\rho/\bar{\rho} \gtrsim 3 - 10$), which requires the use of numerical simulations to compute their properties accurately, the low column density systems may be studied analytically since there exist reliable approximations to study structure formation in the regime of low overdensity. The Lyman-alpha forest arising from these slightly overdense and underdense regions is the subject of this *Letter*.

2. Column Density from the Stationary Phase Integration Around the Peak

We first start with deriving an approximate expression for the column density of an absorption line arising from a density peak in velocity space. Let τ_0 be the Lyman-alpha optical depth for a homogeneous medium at the average cosmological density at redshift z

³We intentionally avoid using the term “clouds” since the forest mostly consists of fluctuations in the intergalactic medium rather than discrete objects.

along a line-of-sight to a distant quasar (see Jenkins & Ostriker 1991). We will consider the range of $z \sim 3$ when hydrogen was in ionization equilibrium with the radiation field which had photoionization rate $\Gamma \equiv 4.3 \times 10^{-12} J_{-21} \text{ s}^{-1}$. J_{-21} , which characterizes the radiation intensity, is assumed to be 0.5. Since the number density of neutral hydrogen is proportional to the square of the density times the recombination coefficient, we can now compute the column density $N_{\text{H I}}$ of a Lyman-alpha absorption line:

$$N_{\text{H I}} \sigma_{\text{Ly}-\alpha} = \frac{\dot{\alpha} \tau_0}{c} \int e^{2(1-\alpha)\xi} dx \quad (1)$$

where $\xi \equiv \ln(1 + \delta)$, δ being the overdensity, and the integral is taken over the spatial comoving coordinate x in the vicinity of the density peak. In this expression we implicitly assume that each Lyman-alpha line is dominated by a single density peak and we ignore peculiar velocity effects. The exact limits of integration are assumed to be unimportant as long as the dominant peak is included. The parameter α measures the deviation from the isothermality; if the recombination coefficient changes with the temperature as $T^{-\beta}$, and the equation of state is $T \sim \rho^\gamma$, then $\Omega_{\text{H I}} \sim \rho^2 T^{-\beta} \sim \rho^{2-\beta\gamma}$ and $\alpha = \beta\gamma/2$. For typical values of $\beta = 0.7$ and $\gamma = 0.5$ (as shown in Hui & Gnedin 1996), the correction for non-isothermality is only $\beta\gamma/2 \lesssim 0.2$. In the following, we will assume $\alpha = 0$, but will allow for a range of temperatures, from 3,000 K to 30,000 K, at every value of density, to account for not only power-law equations of state, but also other relationships between the density and the temperature of the gas. However, we will keep α in our calculations for the sake of generality.

The integral in (1) can be computed using the Stationary Phase method,

$$N_{\text{H I}} \sigma_{\text{Ly}-\alpha} = \frac{\dot{\alpha} \tau_0}{c} e^{2(1-\alpha)\xi_c} \sqrt{\frac{\pi}{-(1-\alpha)\xi_c''}}, \quad (2)$$

where ξ'' is the second derivative of the logarithm of the density with respect to the comoving coordinate along the line-of-sight and the subscript c denotes evaluation at the density peak.

In order to proceed further and compute the column density distribution, we need to know the distribution function of the density and its derivatives. In the linear regime, the distribution function is gaussian, and the calculation can be performed fully analytically. However, we want to apply the approximation (2) to a wider range of overdensities, particularly for underdense regions. We therefore use the lognormal distribution for the density (Bi, Borner, & Chu 1992; Coles, Melott, & Shandarin 1993), which is mainly based upon the assumption that the velocity distribution remains gaussian for larger values of overdensities than the density distribution does. Since the continuity equation in the expanding coordinates can be written as:

$$\frac{d\xi}{dt} = -\frac{1}{a} \frac{\partial v^i}{\partial x^i}, \quad (3)$$

where d/dt denotes the Lagrangian derivative and v is the peculiar velocity, we can see that the density distribution stays close to lognormal (i.e. ξ is normally distributed) as long as v is gaussian.

Since a one-dimensional slice of a three-dimensional gaussian random field is also a gaussian random field, we can use the BBKS formalism (Bardeen et al. 1986) to derive the column density distribution of the low column density Lyman-alpha forest. Let us introduce the quantity g as follows:

$$g \equiv \ln \left(\frac{N_{\text{HI}} \sigma_{\text{Ly}-\alpha} c}{\tau_0 \sqrt{\pi} \dot{a} R_*} \right) + \sigma_0^2 (1 - \alpha) = 2(1 - \alpha)(\xi - \bar{\xi}) - \frac{1}{2} \ln [-R_*^2 (1 - \alpha) \xi''], \quad (4)$$

where the parameters σ_0 , R_* , and γ (which appears below) are defined as in the BBKS paper, and $\bar{\xi} = -\sigma_0^2/2$ is the average value of ξ .

Then the column density distribution (number of absorption lines per unit column density per unit redshift) of the Lyman-alpha forest is given by the following simple expression:

$$\frac{d^2 \mathcal{N}_{\text{Ly}-\alpha}}{dN_{\text{HI}} dz} = \frac{c}{N_{\text{HI}} H_0 \sqrt{\Omega_0 (1+z)^3}} \frac{dn_{\text{pk}}}{dg}, \quad (5)$$

where dn_{pk}/dg is the one-dimensional comoving number density of peaks per unit interval of g , which can be easily computed using the BBKS methodology, and is given by the following expression:

$$\frac{dn_{\text{pk}}}{dg} = \frac{1}{2(2\pi)^{3/2}R_*\sigma_0^3\gamma^2\sqrt{9/5 - \gamma^2(1 - \alpha)}} \int_0^\infty x e^{-Q(g,x)} dx, \quad (6)$$

where

$$Q(g,x) = \frac{1}{2\sigma_0^2(9/5 - \gamma^2)} \left(\frac{9}{5}\Delta^2 - 2x\Delta + \frac{1}{\gamma^2}x^2 \right), \quad (7)$$

and

$$\Delta(g,x) \equiv \xi - \bar{\xi} = \frac{1}{2(1 - \alpha)} \left(g + \frac{1}{2} \ln((1 - \alpha)x) \right). \quad (8)$$

The integral in (6) can be easily computed numerically for a given values of σ_0 and γ .

In order to test our approximation, we compute the exact column densities using the Zel’dovich approximation and Miralda et al. (1996) line identification algorithm and for each identified line we apply the Stationary Phase approximation. We find that the Stationary Phase column density is within a factor of two from and somewhat below (for higher column densities) the exact column density.

Since our approximation assumes the lognormal density distribution, we test it against the Zel’dovich approximation, as shown in Fig.1. We show with open symbols the exact column density distribution (multiplied by the column density to better demonstrate the differences) from our Zel’dovich calculation (see Hui & Gnedin 1996 for details) together with the Stationary Phase calculation using the density distribution from the Zel’dovich approximation (filled triangles). ⁴ The number of absorption lines drops drastically for

⁴The exact computation lies below the Stationary Phase + Zel’dovich approximation at low column density because the Miralda et al. (1996) line identification algorithm significantly underestimates the number of low column density lines (M. L. Norman, private communication).

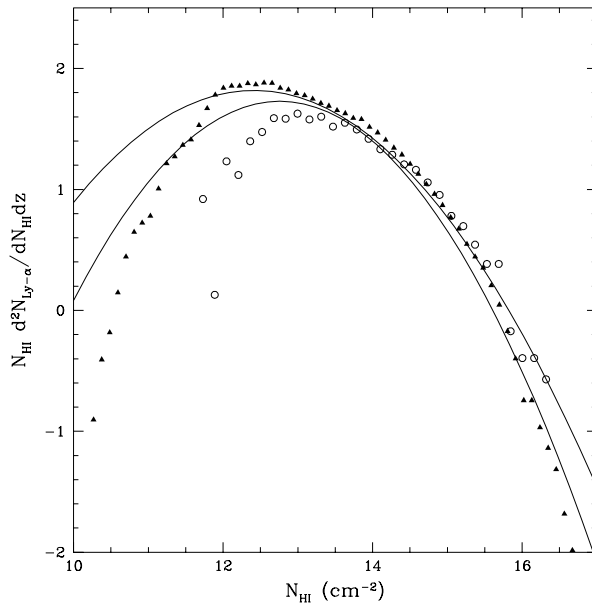


Fig. 1.— The column density distribution for the Standard CDM model with $\sigma_8 = 0.7$ from the full calculation using the Zel’dovich approximation and Miralda et al. (1996) line identification algorithm (*open circles*) and the Stationary Phase calculation using the Zel’dovich approximation for the density distribution (*filled triangles*) versus approximate analytical treatment using the Stationary Phase calculation and the lognormal model for the density field (*solid lines*). The lower line corresponds to the same initial conditions as the Zel’dovich approximation (the same smoothing scale), and the upper line corresponds to the smaller smoothing scale that gives the same rms density fluctuation as the Zel’dovich approximation. The number of lines drops drastically for the simulated distributions at low column densities due to finite resolution.

$N_{\text{HI}} < 10^{12} \text{ cm}^{-2}$ due to the finite resolution of our simulations. The two solid lines show the approximate analytical calculation for two choices of the smoothing scale: the lower curve has the same smoothing as the Zel’dovich approximation, and the upper curve has a smaller smoothing scale so as to have the same rms density fluctuation as the Zel’dovich approximation. In general, we again see that the analytical approximation gives a good guess for the real column density distribution, perhaps, slightly underestimating the column density distribution.

3. Testing the Models

We consider six different models whose parameters are compiled in Table 1. Our treatment only requires three spectral parameters, σ_0 , γ , and R_* . However, for a power spectrum which behaves like k^{-3} at large k , integrals for γ and R_* diverge. The power spectrum, therefore, has to be cut off at some scale. The natural cut-off scale would be the Jeans scale but the power spectrum at scales smaller than it behaves like k^{-7} (Bi et al. 1992), and integrals needed to compute R_* and γ diverge. We, therefore, apply the exponential cut-off at the Jeans scale,

$$P_{\text{gas}}(k) = P_{\text{DM}}(k) e^{-(k/k_J)^2} \quad (9)$$

where

$$k_J \equiv 7.4(\Omega_0(1+z)10^4 \text{ K}/T_J)^{1/2} h \text{ Mpc}^{-1}, \quad (10)$$

but we treat the temperature T_J at which we compute the Jeans scale as an independent parameter not necessarily equal to the gas temperature T_{gas} . We note here that this cut-off of the power spectrum is equivalent to smoothing the one-dimensional density distribution on the scale of Doppler broadening. Even though Doppler broadening does not affect the value of the column density, the identification of a line depends on the value of b

($b = \sqrt{2k_B T/m_p}$ where m_p is the proton mass) as two narrow peaks that are separated by a distance much less than b in velocity space would not be counted as two lines but rather as one line. Since this procedure is somewhat dependent on the line identification algorithm, we use the freedom in T_J as a way to account for differences between different line identification algorithms. We then consider the range of temperatures from 3×10^3 K to 3×10^4 K for both T_J and the gas temperature T_{gas} in our calculations and we put $\alpha = 0$. The range of temperatures at a given density should be enough to cover possible variations for any other reasonable equation of state. We assume $J_{-21} = 0.5$ throughout.

The first two models we consider are standard CDM models, one is with $\sigma_8 = 0.4$ at $z = 0$ and the other is *COBE*-normalized. We use the BBKS transfer function to compute spectral parameters σ_0 , γ , and R_* for this model.

The next three models are the *COBE*-normalized CDM+ Λ models whose transfer functions cannot be fit by the BBKS formula accurately. We therefore compute transfer functions for LCDM models using the linear gravity code similar to (but different from) COSMICS package (Bertschinger 1995) and we use exact transfer functions to compute the spectral parameters. The first LCDM model assumes a small tilt in the primordial power spectrum and 25% of gravity waves added in quadrature as in Kofman, Gnedin, & Bahcall (1993).

Finally, we study the *COBE*-normalized CHDM model with currently favored value of $\Omega_\nu = 0.2$ and no tilt. We use the Ma (1996) transfer function in our calculation. Table 2 lists spectral parameters for the six models at $z = 3$ and $T = 10^4$ K.

Fig.2 shows the computed column density distributions for the above six models where both T_J and T_{gas} independently take values from 3×10^3 K to 3×10^4 K at $z = 3$. We use the old Standard Big Bang Nucleosynthesis value of $\Omega_b h^2 = 0.0125$ for the baryon density in these calculations. We emphasize again that since the temperature of the intergalactic

Table 1: Cosmological Models

| Model | Ω_0 | Ω_Λ | Ω_ν | h | n | σ_8 |
|-------|------------|------------------|--------------|------|------|------------|
| SCDM1 | 1 | 0 | 0 | 0.50 | 1 | 0.40 |
| SCDM2 | 1 | 0 | 0 | 0.50 | 1 | 1.15 |
| LCDM1 | 0.35 | 0.65 | 0 | 0.70 | 0.96 | 0.67 |
| LCDM2 | 0.35 | 0.65 | 0 | 0.70 | 1 | 0.85 |
| LCDM3 | 0.40 | 0.60 | 0 | 0.65 | 1 | 0.84 |
| CHDM1 | 1 | 0 | 0.2 | 0.50 | 1 | 0.76 |

Table 2: Spectral Parameters at $T_J = 10^4$ K

| Model | σ_0 | γ | $R_*(h^{-1} \text{Mpc})$ |
|-------|------------|----------|--------------------------|
| SCDM1 | 1.01 | 0.52 | 0.105 |
| SCDM2 | 2.90 | 0.52 | 0.105 |
| LCDM1 | 1.11 | 0.51 | 0.180 |
| LCDM2 | 1.50 | 0.52 | 0.178 |
| LCDM3 | 1.51 | 0.52 | 0.167 |
| CHDM1 | 1.18 | 0.49 | 0.106 |

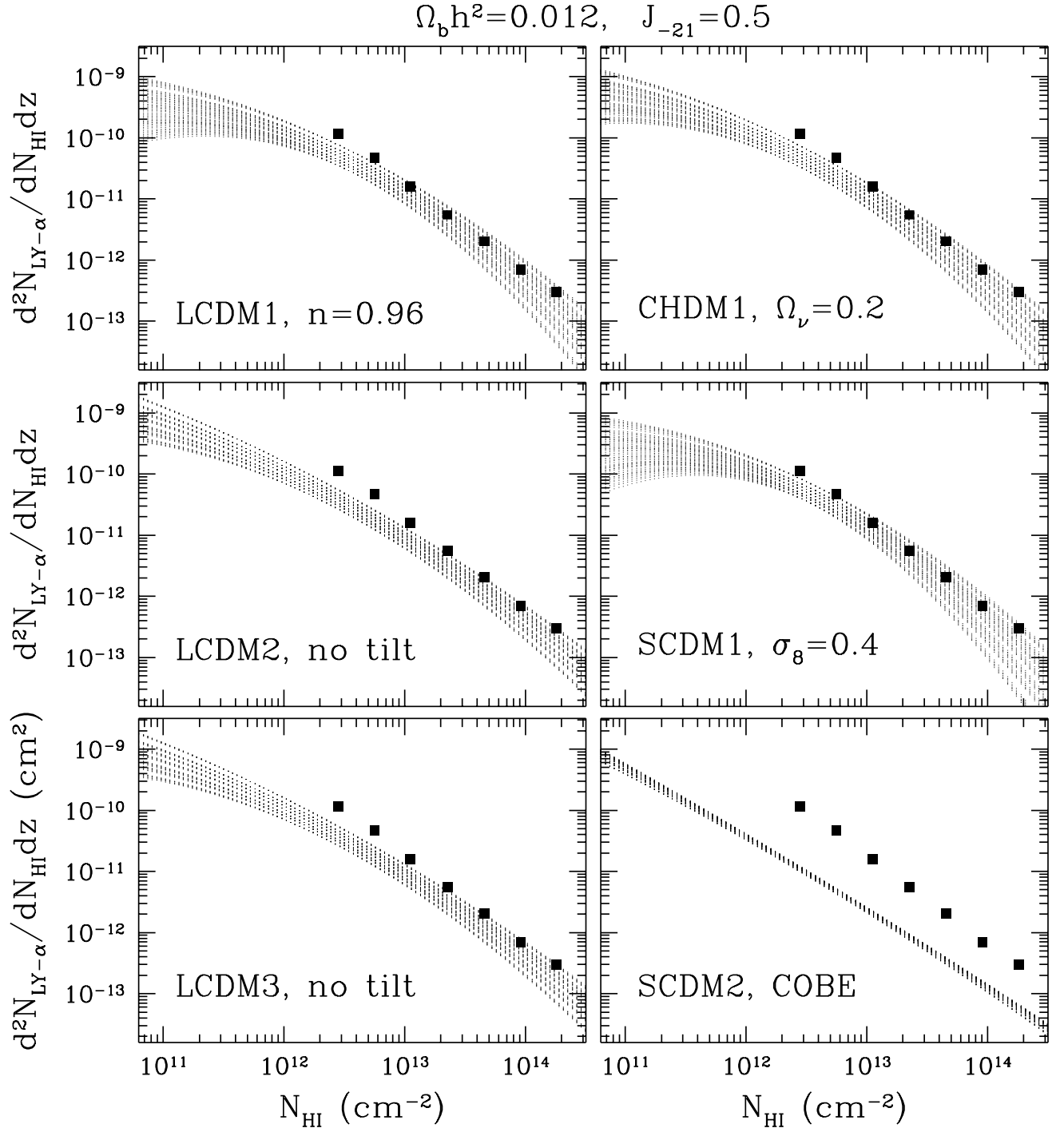


Fig. 2.— Comparison between six cosmological models and observations (*solid squares*) at $z = 3$. The shaded region shows the predicted range for the models with both T_{gas} and T_J taking values between 3×10^3 K and 3×10^4 K.

gas is not known precisely, and it may also depend on local conditions, it is appropriate to consider the hatched area as the region where a more accurate calculation would lie. The width of the hatched area also corresponds to the accuracy of the analytical approximation as can be judged from Fig.1. We also show the observed abundances from Hu et al. (1995) with filled squares. The size of the squares roughly corresponds to the observational uncertainties.

As could be expected, the *COBE*-normalized standard CDM does not fit the data, but the low-amplitude SCDM, slightly tilted LCDM and the CHDM models provide a good fit to the data for low column densities. At higher column densities, $N_{\text{HI}} \gtrsim 10^{14} \text{ cm}^{-2}$, our approximation breaks down since those column densities correspond to significantly overdense regions. The two no-tilt LCDM models produce slightly too few low column density Lyman-alpha systems because their σ_0 is too high and their underdense regions are too underdense; they may be only marginally consistent with observations.

It is remarkable that the column density distribution is by far most sensitive to the value of σ_0 . It is the value of $\sigma_0(T_J = 10^4 \text{ K}) \approx 1.1$ that is responsible for the match with observations for SCDM1, LCDM1, and CHDM1 models. We found that the dependence of the results on other parameters (Ω_0 , h , J_{-21} , T , γ , and R_*) is weaker than dependence on σ_0 , and for any set of those six parameters (within reasonable limits) it is possible to adjust the value of σ_0 to give a good fit to observations.

Finally, we address the question of uncertainty in the baryon density. Recently there have been new determinations of the cosmological baryon density using the high-redshift deuterium measurements giving two contradicting values of $\Omega_b h^2 = 0.006$ (Hogan & Rugers 1996) and $\Omega_b h^2 = 0.024$ (Tytler & Burles 1996). We plot the results for the three best-fit models, LCDM1, CHDM1, and SCDM1, for those two values of the baryon density and $J_{-21} = 0.5$ in Fig.3. We note that the high value for the baryon density improves the

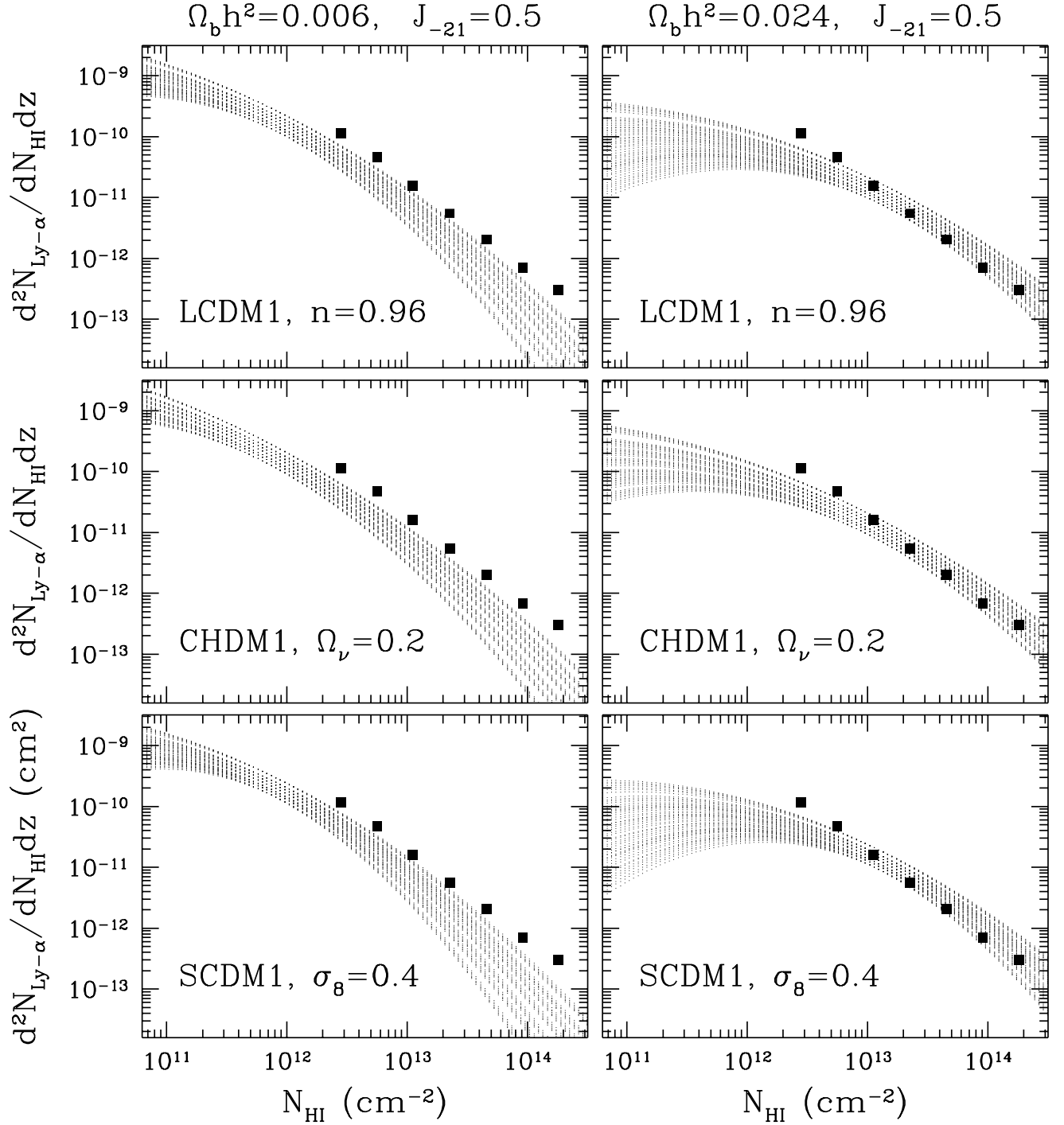


Fig. 3.— Comparison between three best-fit cosmological models and observations for two currently favorable values of the cosmological baryon density.

agreement between the models and the data, while with the low value for the baryon density, the models are only marginally consistent with observations.

4. Conclusions

We have developed an *analytical* method to compute the column density distribution for the Lyman-alpha forest in the low column density limit, $N_{\text{HI}} \lesssim 10^{14} \text{ cm}^{-2}$. We computed the column density distributions for six different cosmological models and found that the standard, *COBE*-normalized CDM model cannot fit the observations of the Lyman-alpha forest at $z = 3$. The amplitude of density fluctuations in that model has to be lowered by a factor of almost 3 to match observations. The *COBE*-normalized CDM+ Λ model with a slight tilt, the *COBE*-normalized CHDM model with $\Omega_\nu = 0.2$, and the low-amplitude Standard CDM model are all in agreement with observations for a range of values for the cosmological baryon density and for the currently favored value of the ionizing background radiation intensity of $J_{-21} = 0.5$. The no-tilt LCDM models without gravity wave contribution produces slightly too few low column density Lyman-alpha systems. We also note that since at high redshift, $z \gtrsim 2$, all cosmological models have similar rate of growth of perturbations on scales of interest (including the CHDM model, since the neutrino free-streaming scale is larger than the characteristic scale for the low column density Lyman-alpha forest), and since the three models, LCDM1, CHDM1, and SCDM1, have similar predictions at $z = 3$, there will be little differences in their predictions at $z = 2$ or $z = 4$. We conclude that, based on the lognormal approximation, the column density distribution alone provides only a weak constraint on currently viable cosmological models unless the physical state of the intergalactic medium is known more precisely from independent observations. A more accurate approximation would also be useful in decreasing the width of the hatched area in Fig.2, which takes into account our ignorance

of the conditions of the intergalactic medium as well as the accuracy of the lognormal approximation.

The computed column density distribution is by far most sensitive to the amplitude of fluctuations at the Jeans scale, σ_0 . We conclude that models with $\sigma_0 \sim 1$ (at $T_J = 10^4$ K and $z = 3$) are capable of reproducing the observational data for a large range of other parameters.

Finally, we note that with the low value for baryon density as inferred by Hogan & Rugers (1996), all of the models tested here are only marginally consistent with observations.

The authors thank Edmund Bertschinger for numerous fruitful discussions and valuable suggestions. We are also grateful to Sergei Shandarin for very helpful comments. This work was supported in part by the NSF grant AST-9318185.

REFERENCES

- Bardeen, J. M., Bond, J. R., Kaiser, N., & Szalay, A. S. 1986, *ApJ*, 304, 15
- Bertschinger, E. 1995, astro-ph 9506070
- Bi, H. G., Borner, G., & Chu, Y. 1992, *Å*, 266, 1
- Cen, R. Y., Miralda-Escude, J., Ostriker, J. P., & Rauch, M. R. 1994, *ApJ*, 437, L9
- Coles, P., Melott, A. L., & Shandarin, S. F., 1993 *MNRAS*, 260, 765
- Hernquist, L., Katz, N., Weinberg, D. H., & Miralda-Escude, J. 1995, *ApJ*, 457, L51
- Hogan, C., & Rugers, M. 1996, astro-ph 9603084
- Hu, E., Kim, T., Cowie, L. L., & Songalia, A. 1995, *AJ*, 110, 1526
- Hui, L., & Gnedin, N. Y. 1996, in preparation
- Jenkins, E. B., & Ostriker, J. P. 1991, *ApJ*, 376, 33
- Kofman, L. A., Gnedin, N. Y., & Bahcall, N. A. 1993, *ApJ*, 413, 1
- Ma, C. 1996, *ApJ*, 471, in press (astro-ph 9605198)
- Miralda-Escude, J., Cen, R. Y., Ostriker, J. P., & Rauch, M. 1996, *ApJ*, submitted (astro-ph 9511013)
- Tytler, D., & Burles, S. 1996, astro-ph 9606110
- Zhang, Y., Meiksin, A., Anninos, P., & Norman, M. L. 1996, astro-ph 9601130